UJEAS

UNIZIK JOURNAL OF ENGINEERING AND APPLIED SCIENCES

UNIZIK Journal of Engineering and Applied Sciences 6(5), December (2026), 4207-4219
Journal homepage: https://journals.unizik.edu.ng/index.php/ujeas
PRINT ISSN: 2992-4383 || ONLINE ISSN: 2992-4391

Thermodynamic and Economic Assessment of Pre- and Post-Pump Internal Heat Exchanger Integration in an Ammonia–Water Absorption Refrigeration Cycle

Osita Benedict Agbatah
Environmental Science, Enugu State University of Science and Technology, Agbani, Enugu, Nigeria.
Chibuzo John Onyia
Department of Chemical Engineering, Chukwuemeka Odumegwu Ojukwu University, Uli, Anambra State, Nigeria.
Abang Sunday Scott Igwe
Mathematics department, Enugu state University of science and Technology, Agbani, Enugu, Nigeria
Chiedozie Joshua Onoh
Research Department, National Centre for Technology Management (NACETEM), P.M.B 12, Obafemi Awolowo University (O.A.U.), Ile-Ife, Osun State, Nigeria.
Chukwudi Christian Okoli
Mechanical Engineering Department, Nnamdi Azikiwe University, Awka, Anambra State, Nigeria

**Corresponding Author's E-mail: buzors78@outlook.com*

Abstract

This study compares three steady-state simulations of an ammonia–water absorption refrigeration (AAR) cycle: a baseline without an internal heat exchanger (IHE), an IHE placed before the solution pump, and an IHE placed after the pump. The NRTL–Redlich–Kwong (NRTL–RK) property method was selected for the ammonia–water mixture. At a nominal cooling duty of 600 kW, the reported coefficient of performance (COP) values were 0.3762, 0.4028, and 0.5165 for the baseline, pre-pump, and post-pump configurations, respectively. Relative to the baseline, the pre-pump and post-pump arrangements increased COP by approximately 7.0% and 37.3%, respectively. The corresponding reported reboiler duties were 1593, 1488, and 1160 kW, indicating a 27.2% reduction for the post-pump configuration relative to the baseline. The reported circulation rate was 6552 kg h^{-1}. A preliminary area-based estimate gives an IHE area of approximately 7.98 m^2 and an indicative area cost of £797.50 under an assumed unit cost of £100 m^{-2}. Separately, the manuscript reports an annual distillation-column operating cost of £3.7 million; this figure cannot be reconciled with the available cost assumptions and is therefore treated as provisional rather than directly comparable with the exchanger estimate. The results support the post-pump arrangement thermodynamically within the stated simulation conditions, while further validation, consistent equipment costing, and sensitivity analysis are required before industrial economic feasibility can be established.

Keywords: ammonia–water absorption refrigeration; internal heat exchanger; coefficient of performance; Aspen HYSYS; thermodynamic simulation; preliminary cost estimation

1. Introduction

Ammonia–water absorption refrigeration (AAR) is a thermally driven refrigeration technology in which ammonia acts as the refrigerant and water as the absorbent. Compared with water–lithium bromide systems, ammonia–water cycles can serve sub-zero refrigeration duties, making them relevant to food preservation, cold storage, and selected process applications. Their performance depends on operating temperatures and pressures, solution concentration, component effectiveness, and the recovery of sensible heat within the cycle (Caldas et al., 2021; Wang et al., 2021). Because the generator or desorber commonly accounts for a substantial thermal input, improving internal heat recovery is an important route to reducing external heat demand and increasing the coefficient of performance (COP).

Previous work has examined heat integration and optimization in ammonia–water systems. For example, Chen et al. (2017) reported that selected heat-integration modifications could increase COP by up to 22% under the

conditions studied. Chávez-Islas et al. (2009) formulated an optimization framework that considered heat-exchanger choices, refrigeration constraints, and annualized capital and operating costs. These studies demonstrate that cycle configuration and heat recovery can materially affect performance; however, their results do not, by themselves, establish the relative performance of placing an internal heat exchanger specifically before versus after the solution pump under a common set of simulation assumptions.

A targeted gap therefore remains in the comparative evaluation of pre-pump and post-pump internal heat exchanger (IHE) integration using a consistent ammonia–water cycle model and a common cooling-duty basis. In particular, thermodynamic gains need to be reported alongside transparent cost assumptions, because an equipment-area estimate and a plant-wide annual operating cost represent different economic quantities and cannot be compared directly without a defined cost boundary, capacity basis, and annualization method.
This study addresses that gap by comparing a baseline AAR cycle with pre-pump and post-pump IHE configurations simulated in Aspen HYSYS using the NRTL–RK property method. The objectives are to: (i) compare COP and reboiler duty at a nominal cooling duty of 600 kW; (ii) report the circulation rate and available heat-exchanger outlet temperatures; (iii) estimate the IHE area and indicative area-based cost using explicitly stated assumptions; and (iv) examine the reported distillation feed-tray/reflux result while identifying unresolved cost and data-consistency limitations. The scope is a steady-state simulation comparison, not an experimentally validated design or a complete discounted-cash-flow assessment.

2.0 Materials and methods

A steady-state process model was developed in Aspen HYSYS for an ammonia–water absorption refrigeration cycle. Three configurations were considered: (1) no internal heat exchanger, (2) an internal heat exchanger upstream of the solution pump, and (3) an internal heat exchanger downstream of the solution pump. The nominal cooling duty was held at 600 kW to provide a common basis for comparing the configurations. The working fluid was an ammonia–water mixture, and the NRTL–RK property method was selected to represent liquid-phase non-ideality and vapour-phase behaviour. The available manuscript records do not provide a complete model-validation dataset; consequently, the reported outputs should be interpreted as simulation results rather than independently validated plant performance.

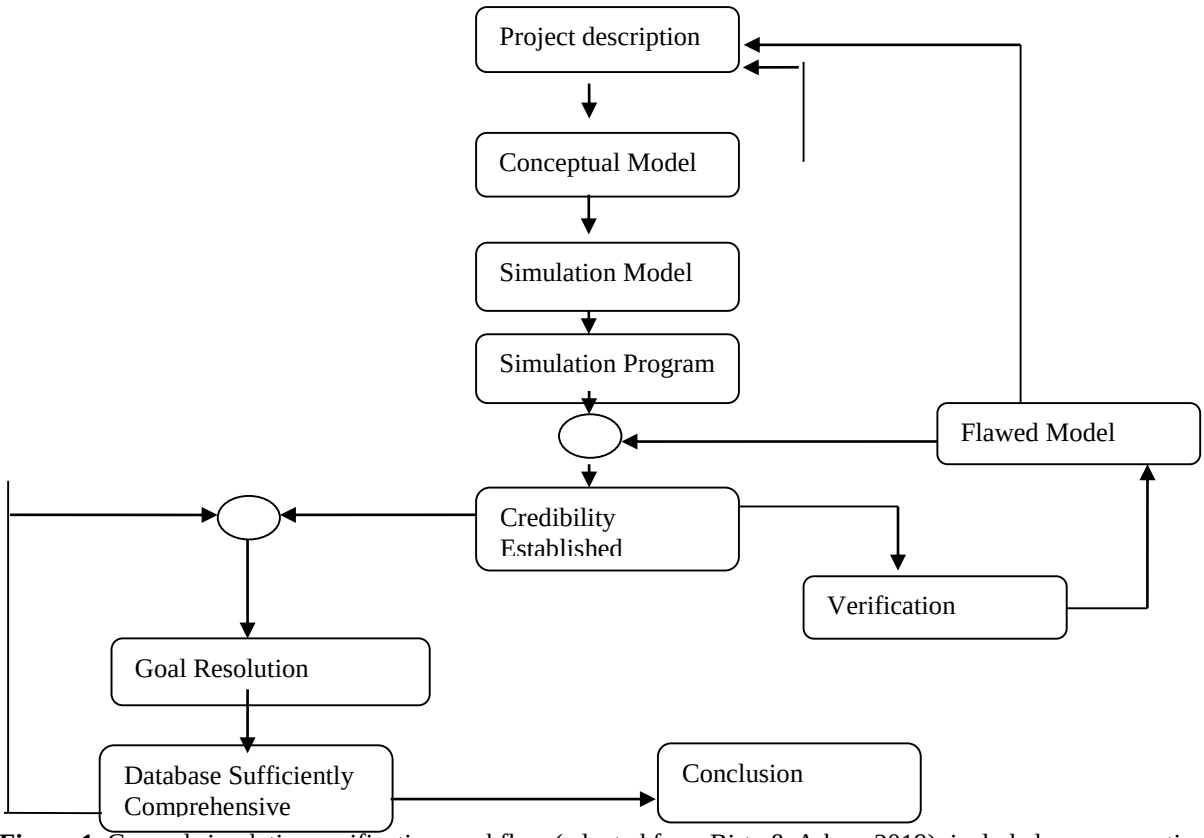


Figure 1. General simulation verification workflow (adapted from Birta & Arbez, 2019); included as a supporting workflow rather than as part of the AAR cycle mod

2.1 Ammonia–water absorption refrigeration cycle

The model represents a single-effect ammonia–water absorption refrigeration loop comprising a desorber/generator, condenser, expansion valve, evaporator, absorber, solution pump, and optional internal heat exchanger. The cycle is assessed under three heat-exchanger configurations. Figure 2 presents the process-flow representation used for the AAR model; the detailed stream and equipment specifications are provided in the accompanying simulation flowsheets in the Appendix.

AAR system involves a vapour absorption refrigeration structure. An ammonia water solution (NH_3/H_20) is pumped into the short cut distillation column (desorber) where the process commences.

Ammonia is the refrigerant (more volatile component), while water is the absorbent. Heat supplied to the desorber separates ammonia-rich vapour from the solution. After condensation and throttling, ammonia evaporates while absorbing the cooling load. The vapour is then absorbed into the water-rich solution, and the solution pump returns the liquid to the high-pressure side. The IHE transfers sensible heat between process streams; its location relative to the pump is the principal configuration variable examined here.

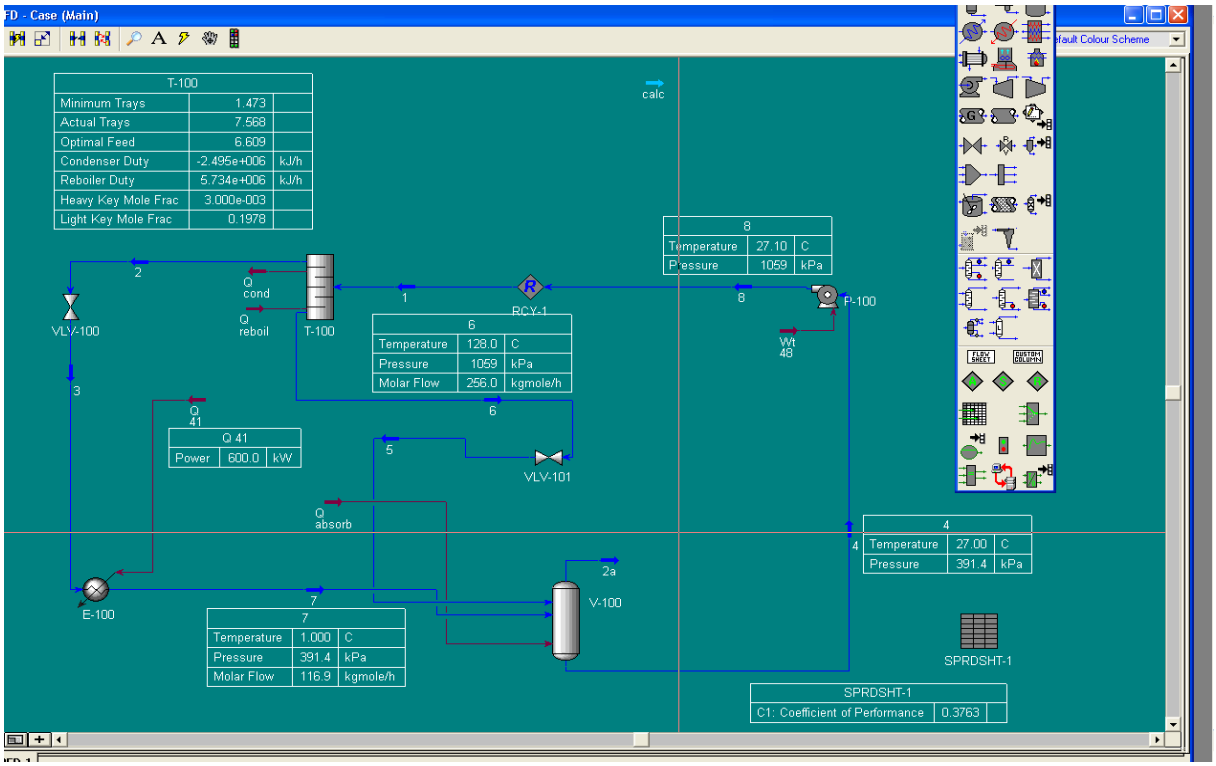


Figure 2. Aspen HYSYS process-flow diagram of the ammonia–water absorption refrigeration cycle (baseline configuration).

The NH_3/H_20 solution is fed into the desorber, with a mass fraction of 0.45:0.55,an assumed mass flow of 5000kg/h and pressure of 1059kPa. Heat is supplied to boil off the NH_3 from the solution. Because water has a higher saturation temperature, water vapour gets condensed into the water particles that drip downwards. The light key refrigerant in the gaseous state continues to rise up. The resulting vapour contains about 0.3% of the heavy key, due to the strong affinity between ammonia and water (Wang, 2021). The vapour is condensed by the condenser and further cooled upon passing through the pressure reducing valve to the evaporator. The core refrigeration (cooling effect) occurs in the evaporator. The ammonia absorbs heat from the product to be cooled and vaporises, and moves on to the absorber (V-100). In the absorber, containing water as the absorbent, which is unsaturated, that is: it can absorb more of the refrigerant, readily absorbs the ammonia from the evaporator forming a strong NH_3/H_20 solution, which is delivered to pump. The pressure of the two streams entering the absorber from the evaporator (temperature of 1^0C) and desorber bottom (reboiler temperature of 128^0C) respectively is set to be the same in order to prevent back flow. The pump(P-100) pumps the liquid to the heat exchanger at high pressure. The heat exchanger is placed after the pump (which gives the system the highest coefficient of performance).

The heat exchanger heats the liquid by means of heat transfer via the tube and the shell in the heat exchanger without adding energy to the process (Wang, 2021). This is recycled back to the desorber. It is observed that upon introduction of the heat exchanger the power required by the reboiler, that is $Q_{Reboiler}$ reduces. The cycle continues repeatedly cooling the stored products. The short cut distillation is replaced with a real distillation column.

2.1.1Comparison of Coefficient of Performance, COP.

The coefficient of performance is used as a yardstick in measuring the performance of a refrigeration cycle. Defined as the ratio of the heat removed to the work expended.

COP = Q̇_evap / (Q̇_reboiler + Ẇ_pump)

where Q̇_evap is the evaporator cooling duty (kW), Q̇_reboiler is the heat supplied to the desorber/reboiler (kW), and Ẇ_pump is the solution-pump power input (kW).

The COP values were recalculated from the stated 600 kW cooling duty and the listed reboiler and pump duties using COP = Q̇_evap/(Q̇_reboiler + Ẇ_pump). This gives 0.3762, 0.4028, and 0.5165 for the baseline, pre-pump, and post-pump configurations, respectively. These recalculated values differ slightly from the original reported baseline and post-pump values, so the arithmetic has been made consistent with the stated energy inputs.

COP *for process without heat exchanger:*

$$600\text{KW} = \frac{0.3762}{(1593 + 1.686)\ \text{KW}}$$

COP for process with heat exchanger before the pump:

$$600\text{KW} = \frac{0.4028}{(1488 + 1.718)\ \text{KW}}$$

COP for process with heat exchanger after the pump:

$$600\text{KW} = \frac{0.5165}{(1160 + 1.686)\ \text{KW}}$$

The post-pump IHE configuration has the highest reported COP and lowest reboiler duty of the three cases. This is a comparison at the specified simulation conditions; it does not establish that the same ranking will hold at all operating pressures, solution concentrations, exchanger effectiveness values, or cooling-water temperatures.

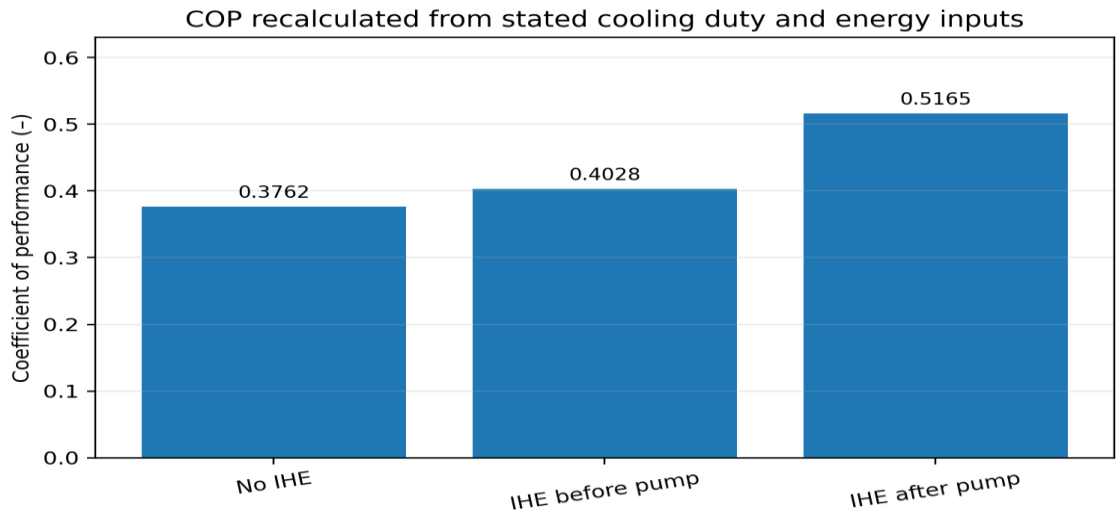


Figure 3. COP recalculated from the stated cooling duty and energy inputs for the baseline, pre-pump IHE, and post-pump IHE configurations.

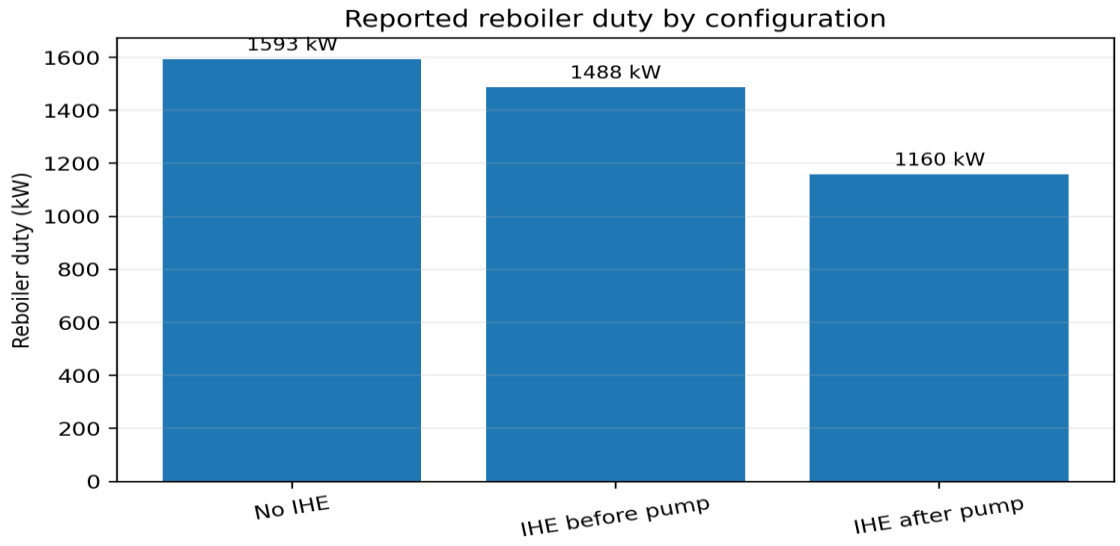


Figure 4. Comparison of reported reboiler duties for the three configurations

Quantitative comparison: relative to the baseline, the pre-pump IHE case increases COP by 7.0% and lowers reboiler duty by 6.6%; the post-pump IHE case increases COP by 37.3% and lowers reboiler duty by 27.2%. These percentages are calculated from the values reported in the manuscript and are not independent simulation results.

$Q_{reboiler}$ for process without heat exchanger**: 1593kW**
$Q_{Reboiler}$ for process with heat exchanger before the pump**: 1488kW**
$Q_{Reboiler}$ for process with heat exchanger after the pump**: 1160kW**

2.1.2 Thermodynamic Property Method

Thermodynamic property-method selection affects predicted phase equilibrium, enthalpy, and equipment duties. The present model uses the NRTL–RK method, combining the Non-Random Two-Liquid activity-coefficient model for liquid-phase non-ideality with the Redlich–Kwong equation of state for vapour-phase calculations. Because ammonia–water equilibrium is central to the generator and absorber, the property method and its binary interaction parameters should be documented and validated against relevant experimental vapour–liquid-equilibrium data in future work.

The NRTL–RK method was retained for all three configurations so that the comparison was made on a consistent thermodynamic basis. No independent validation against measured cycle data is reported in the available model; accordingly, numerical precision in the software output should not be mistaken for demonstrated predictive accuracy.

3.0 Result and Discussion

At a nominal evaporator cooling duty of 600 kW, the reported circulation mass flow rate (stream 1) was 6552 kg h^{-1}. The available model output does not include enough stream-by-stream mass and energy data to independently close every component balance.
Reported circulation mass flow rate = 6552 kg h^{-1}.

Internal heat exchanger outlet temperatures
The reported outlet temperatures are listed below. Stream labels are retained from the original HYSYS model; because the stream definitions are not fully reproduced in the manuscript, the values are presented as reported rather than assigned additional physical interpretations.

Temperature (^{0}C)	**Stream (Heat Exchanger before pump)**
39.72	4A
119.7	6A

Temperature (^{0}C)	**Stream (Heat Exchanger after pump)**
75.25	8
70.76	6A

Preliminary internal heat exchanger area and cost estimate

The preliminary area estimate uses the overall heat-transfer conductance UA reported by HYSYS and an assumed overall heat-transfer coefficient U = 1500 W m^{-2} K^{-1}. The area is calculated from A = UA/U after unit conversion. This is an assumption-based sizing estimate, not a detailed mechanical design; a final design would require terminal temperatures, LMTD correction, pressure drop, fouling allowance, material specification, and design-code requirements.

For unit consistency, 1500 W m^{-2} K^{-1} = 5400 kJ h^{-1} m^{-2} K^{-1}.

A temperature difference of 1 °C is numerically equal to 1 K.
1 °C = 1 K = 1.8 °F = 1.8 °R

Assumed overall heat-transfer coefficient: $U = \frac{5400 \text{ kJ } h^{-1} m^{-2} K^{-1}.}{1000WC}$

Reported overall conductance: UA = 4.307×10^4 kJ h^{-1} K^{-1}.

Calculated area: A = UA/U = $(4.307 \times 10^4)/(5400)$ = 7.98 m^2.

The resulting area estimate is approximately 7.98 m^2.

The original simulation notes report a tube length of 0.7901 m. This value is retained as a model output and should be checked against a detailed exchanger geometry and design specification.

E-101		
Duty	1.555e+006	kJ/h
Tube Side Feed Mass Flow	6549	kg/h
Shell Side Feed Mass Flow	4558	kg/h
Tube Inlet Temperature	27.11	C
Tube Outlet Temperature	75.25	C
Shell Inlet Temperature	128.0	C
Shell Outlet Temperature	70.85	C
Tube length	0.7901	m
Overall U	5403	kJ/h-m2-C
Heat Trans. Area Per Shell	7.943	m2

Figure 5. Internal heat exchanger sizing basis: area calculated from the reported UA and assumed overall heat-transfer coefficient.

Furthermore, assuming a specific price for a m^2 heat exchanger area. The ideal material for the heat exchanger been designed will depend on various factors such as:

- Resistance to operating temperature and pressure
- Cost
- Availability
- Compatibility of material with fluid
- Wear and tear

Material selection should consider ammonia compatibility, corrosion resistance, operating pressure and temperature, fabrication, availability, and lifecycle cost (Sinnott & Towler, 2020; Thulukkanam, 2013). The present manuscript assumes stainless steel and a unit area cost of £100 m^{-2}; this is an illustrative assumption and is not a current vendor quotation.

Copper and copper-containing alloys are generally unsuitable for ammonia service because of compatibility concerns; the final material choice should be confirmed against applicable standards and supplier guidance.

Using the assumed unit area cost of £100 m^{-2}, the estimated bare-area cost is:

$$\text{Cost} = 7.975\ m^2 \times £100\ m^{-2} = £797.50.$$

The £797.50 figure is only a preliminary area-based estimate. It excludes pressure-vessel design, headers, supports, fabrication, installation, instrumentation, insulation, maintenance, contingency, and project-specific factors; it must not be interpreted as a complete installed exchanger cost.

Distillation feed location and reflux ratio: reported results and consistency

The manuscript also reports a McCabe–Thiele-based assessment of feed location and reflux ratio for the distillation/rectification section. Such an analysis can indicate separation trade-offs, but its reliability depends on the equilibrium model, feed condition, target product purities, tray efficiency, and consistent definitions of minimum and operating reflux ratios. The available results are summarized cautiously because the underlying stagewise data and cost calculation workbook are not supplied.

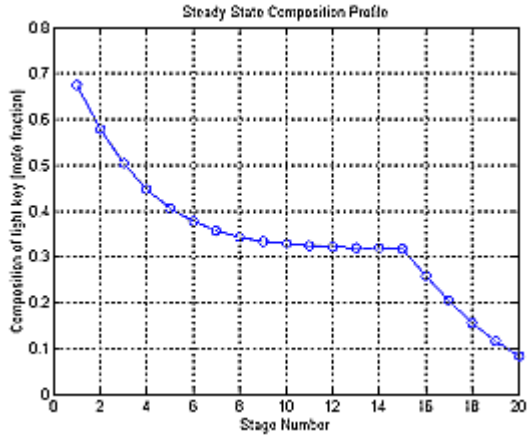


Figure 6. Reported effect of feed-tray location on light-key separation in the distillation column (source-model output; axes and operating conditions should be stated on the original plot).

The reported trend is that moving the feed location downward worsens light-key separation under the simulated conditions. Reflux ratio is defined as $R = L_0/D$, where L_0 is the liquid reflux returned to the column and D is the distillate flow rate. Increasing reflux generally improves separation but increases energy demand; an economic optimum requires a consistent balance between tray/capital cost and reboiler/condenser duty.

The manuscript reports an optimum feed location of approximately tray 8 and an external reflux ratio of 0.22, alongside an annual cost of £3.7 million. However, it also gives an iteration range of 0.016–0.040 and does not provide a transparent cost equation, annual operating hours, energy price, column throughput, or a reconciliation of the reflux-ratio values. Therefore, the tray/reflux result and £3.7 million annual cost are provisional and cannot be considered independently reproduced or validated from the information presented.

The original cost assumptions include £850 per tray and an annual power-related figure of £8000, but the relationship between these values, the stated 0.04 kW h^{-1} consumption, the number of trays, and the reported £3.7 million annual cost is not sufficiently specified. The economic model should be recalculated with a clearly stated

basis (currency year, plant capacity, annual operating hours, energy prices, annualization factor, and included cost items).

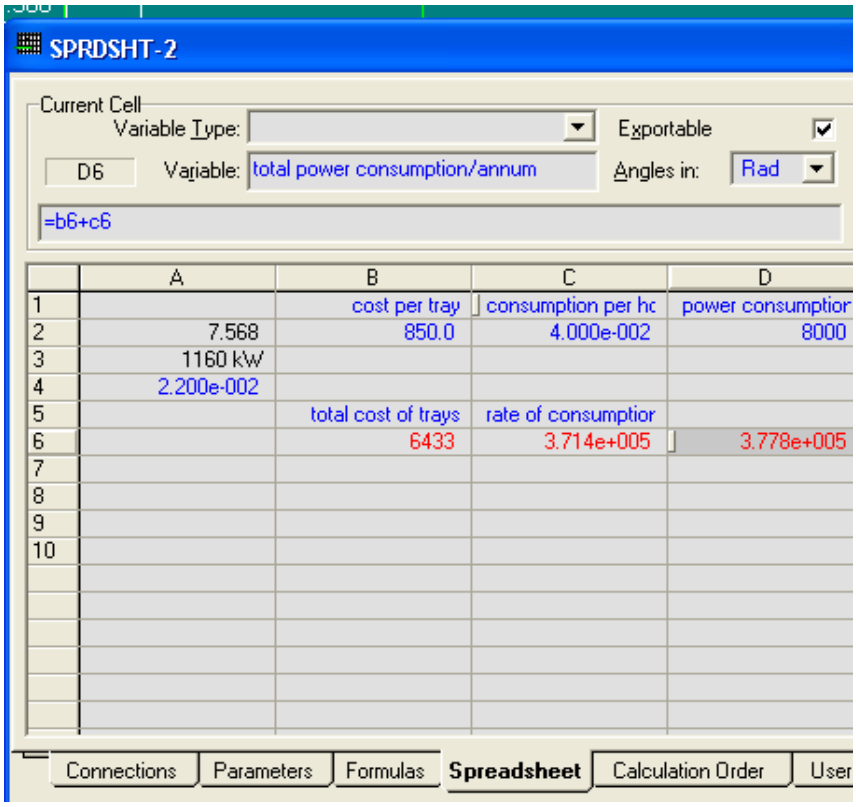


Figure 7. Reported feed-tray/reflux-ratio optimization results; the plot should identify the objective function, reflux-ratio range, and tray-count basis.

The reported tray-8 result should be treated as a preliminary model indication only. In particular, the reported optimum reflux ratio of 0.22 is inconsistent with the stated iteration range of 0.016–0.040; this discrepancy must be resolved from the original simulation data before the result is used for design or costing.

3.1 Discussion and Limitations

The reported results show a consistent thermodynamic advantage for the post-pump IHE case within the selected model: it has the largest COP and lowest reboiler duty. The COP improvement is consistent with the expected benefit of internal sensible-heat recovery, but its magnitude is specific to the operating conditions and heat-exchanger representation used in the simulation. The available manuscript does not report sensitivity analyses for pressure, ammonia mass fraction, exchanger effectiveness, or heat-transfer coefficient, and it does not provide independent experimental validation. These omissions limit generalization beyond the modeled case.

The economic findings are less conclusive than the thermodynamic findings. The £797.50 estimate is derived from an assumed area cost of £100 m^{-2} and an estimated area of about 7.98 m^2; it is a bare-area estimate rather than a complete purchase or installed cost. The £3.7 million figure refers to a separate annual distillation-column cost, but the manuscript does not document a reproducible calculation linking tray cost, energy consumption, annual operating hours, and utility prices to that total. The two figures have different cost boundaries and time bases and must not be compared as equivalent quantities. In addition, the stated reflux-ratio optimum of 0.22 conflicts with the stated iteration range of 0.016–0.040. The source calculations must be checked before any definitive economic optimum is claimed.

Future work should validate the simulation against published or experimental ammonia–water equilibrium and cycle data; solve all three configurations at identical boundary conditions; tabulate component mass and energy balances; and conduct sensitivity analyses of key operating variables. A consistent techno-economic model should report equipment purchase and installation costs, annual utility costs, maintenance, plant capacity, annual operating hours, currency year, and annualization assumptions.

Nomenclature

A — heat-transfer area (m^2).

COP — coefficient of performance (dimensionless).

D — distillate flow rate ($kg\ h^{-1}$).

L_o — liquid reflux flow rate returned to the distillation column ($kg\ h^{-1}$).

$\dot{Q}$_evap — evaporator cooling duty (kW).

$\dot{Q}$_reboiler — heat supplied to the desorber/reboiler (kW).

UA — overall heat-transfer conductance ($kJ\ h^{-1}\ K^{-1}$).

U — overall heat-transfer coefficient ($kJ\ h^{-1}\ m^{-2}\ K^{-1}$).

$\dot{W}$_pump — solution-pump power input (kW).

R — external reflux ratio, L_o/D (dimensionless).

IHE — internal heat exchanger; AAR — ammonia–water absorption refrigeration.

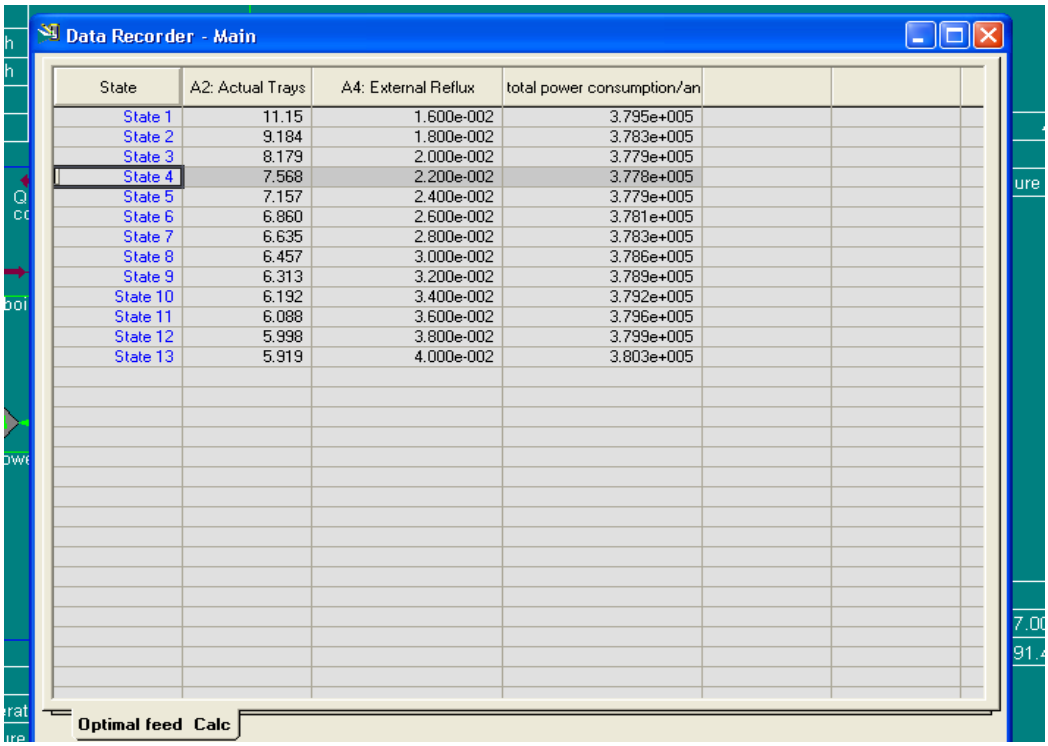
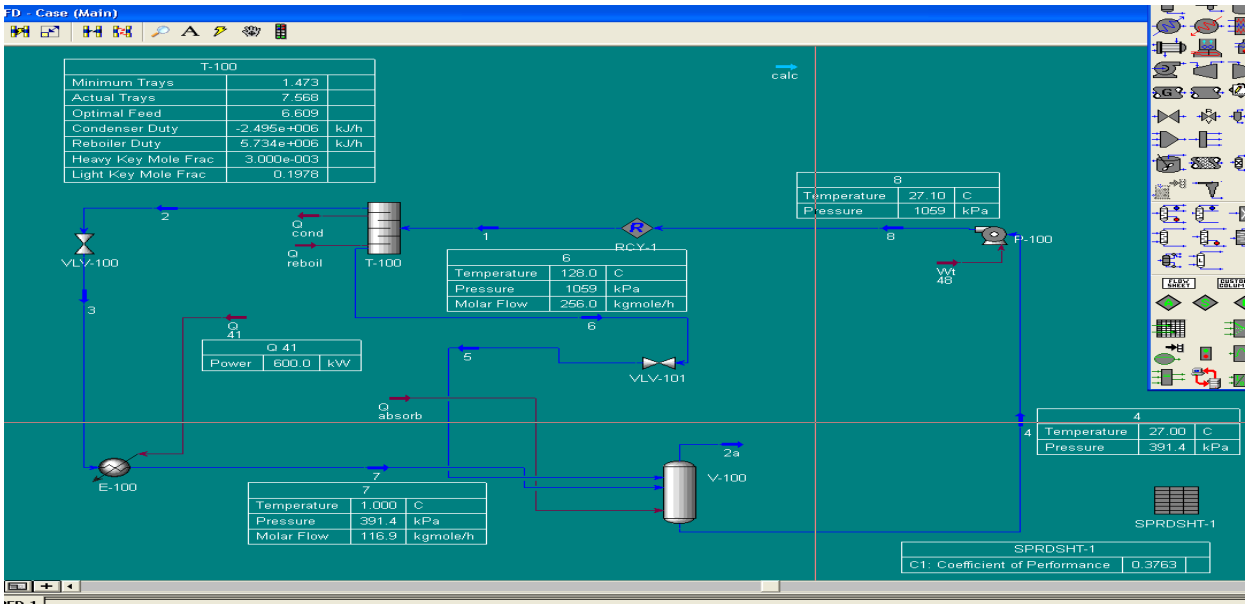


Figure 8. Reported economic optimization output for feed location and reflux ratio; annual-cost values require recalculation and reconciliation with the stated assumptions.

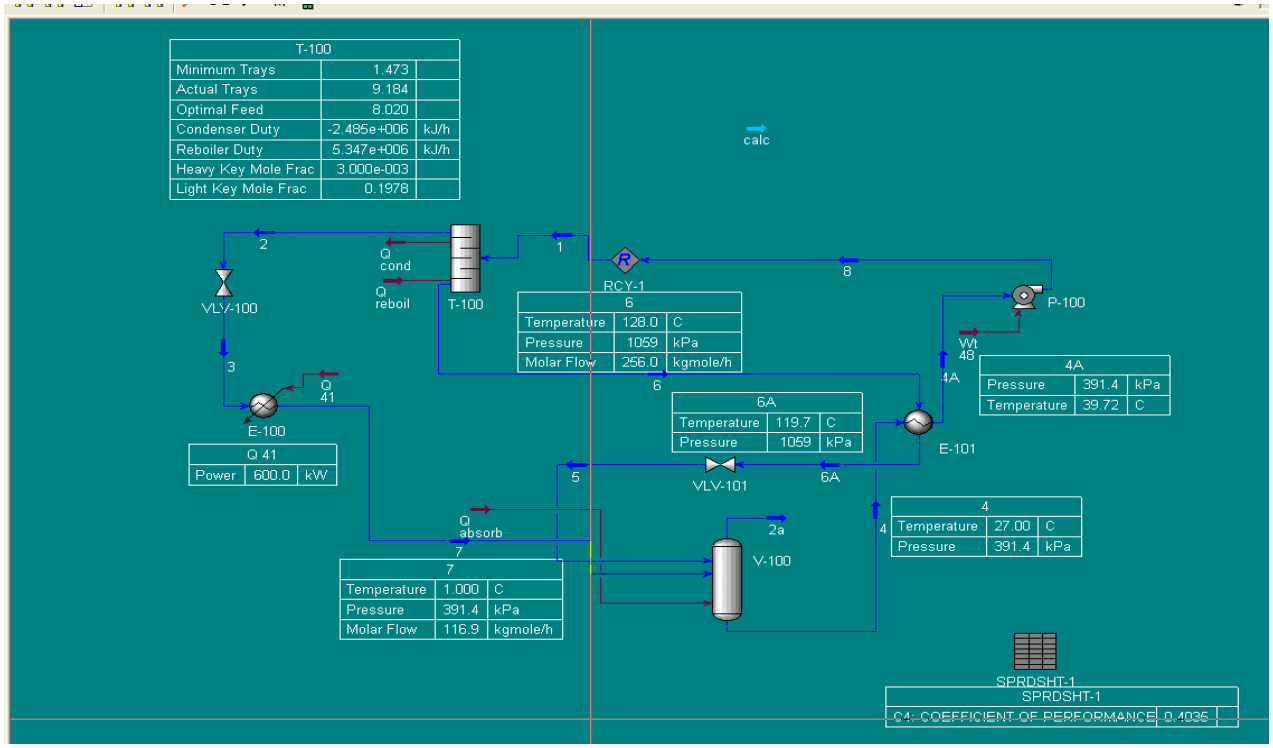
4.0. Conclusion

For the three steady-state cases reported at a 600 kW cooling duty, the post-pump IHE configuration produced the highest COP (0.5165) and lowest reboiler duty (1160 kW), compared with COP values of 0.4028 and 0.3762 and reboiler duties of 1488 and 1593 kW for the pre-pump and baseline cases, respectively. Relative to the baseline, the post-pump arrangement increased COP by about 37.3% and reduced reboiler duty by about 27.2%. The reported circulation rate was 6552 $kg\ h^{-1}$. An assumption-based exchanger area estimate of approximately 7.98 m^2 gives a bare-area cost of £797.50 at £100 m^{-2}, but this is not an installed equipment cost. The separate £3.7 million annual distillation cost cannot be validated from the documented assumptions, and the stated optimum reflux ratio conflicts with the iteration range. Thus, the thermodynamic comparison favours post-pump IHE integration under the modeled conditions, whereas a definitive economic-feasibility claim requires validated cycle data, a reconciled distillation calculation, and a transparent capital and operating cost model.

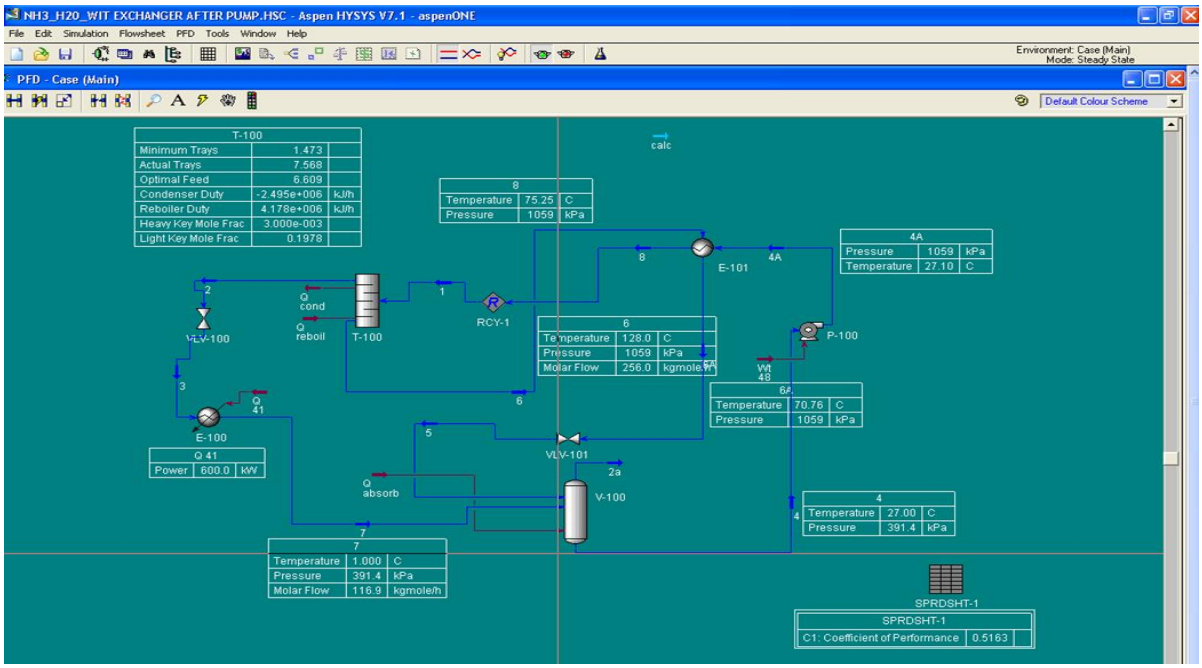
Appendix.



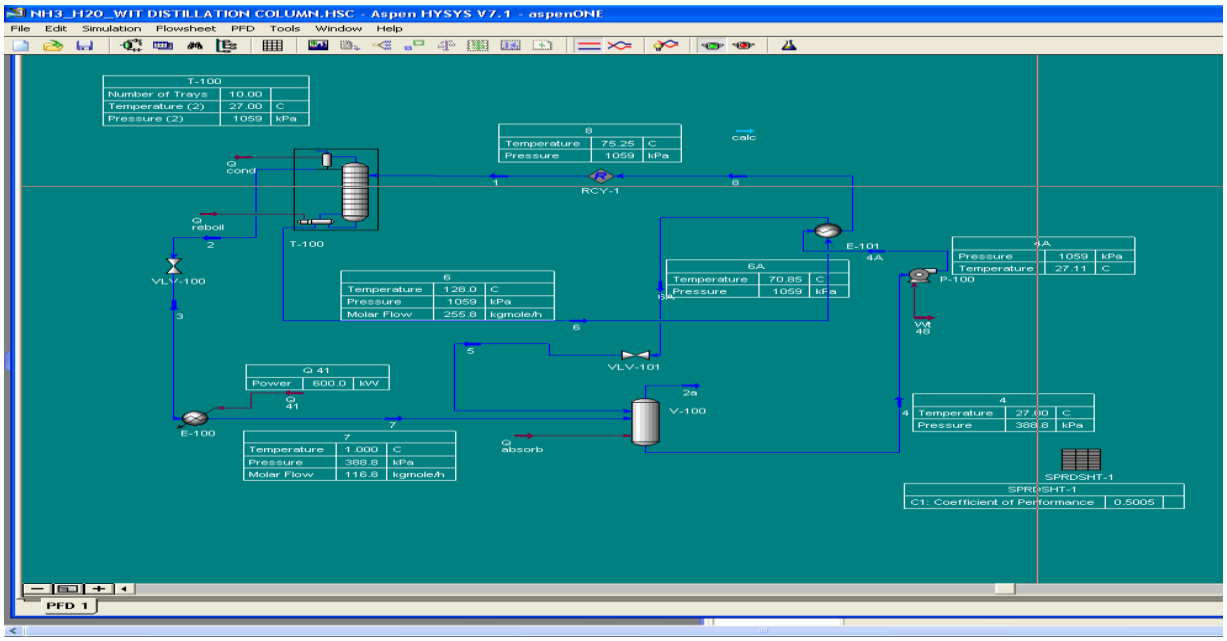
1. Appendix A. Process-flow diagram for the baseline AAR configuration without an internal heat exchanger.



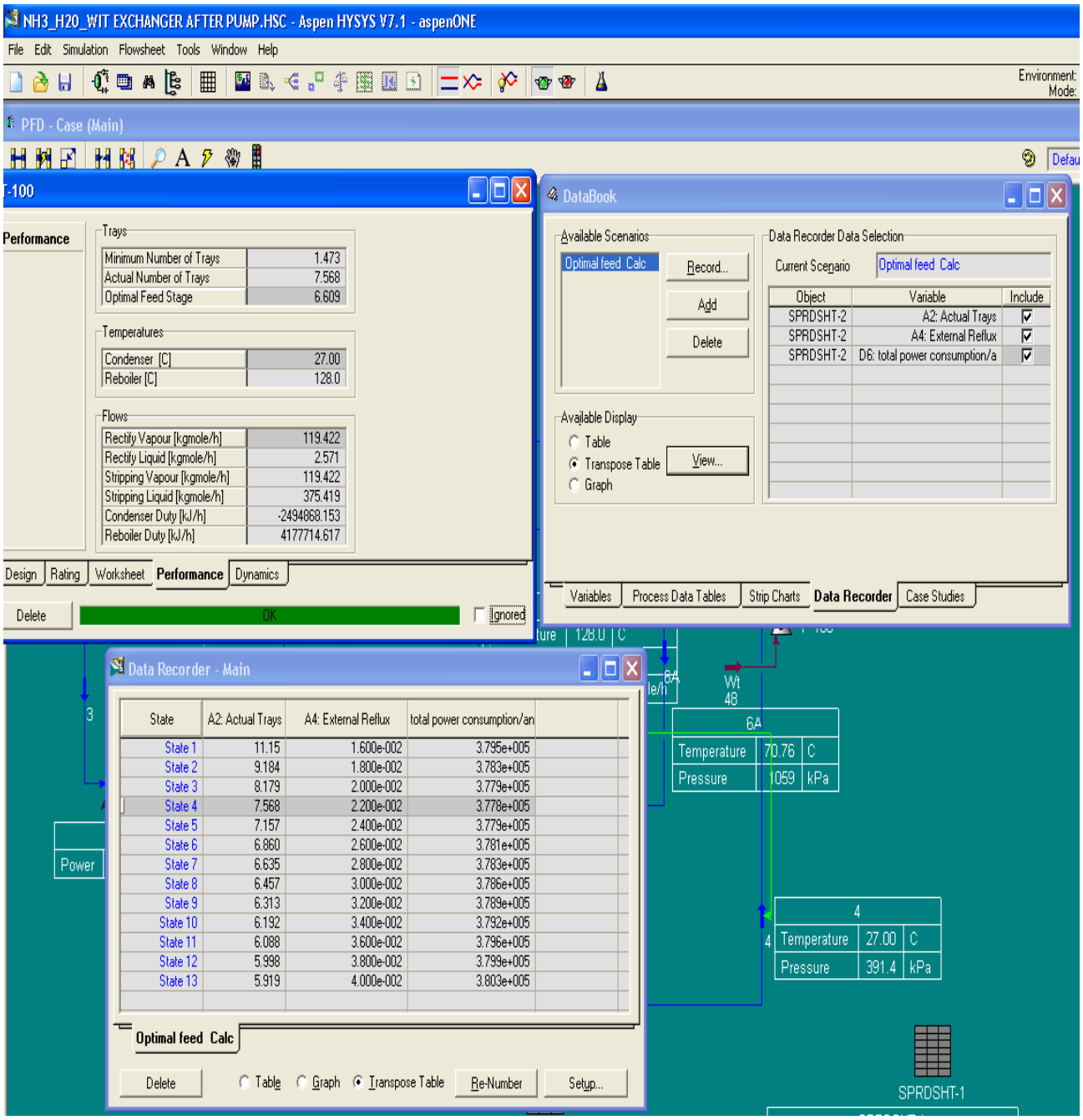
2. Appendix B. Process-flow diagram with the internal heat exchanger placed before the solution pump.



3. Appendix C. Process-flow diagram with the internal heat exchanger placed after the solution pump.



4. Appendix D. Process-flow diagram incorporating the distillation column.



5. Appendix E. Source-model calculation sheet for the reported feed-location optimization.

Declaration of Generative AI and AI-assisted technologies in the writing process

During the preparation of this manuscript, the authors used DeepSeek to assist with language refinement, grammar correction, and clarity enhancement of the text. The tool was employed solely to improve readability and ensure consistent scientific terminology. All intellectual content, including the research design, methodology, data analysis, interpretation, and final conclusions, remains the original work of the authors. The use of AI did not influence the scientific integrity or originality of this research. After using DeepSeek, the authors reviewed and edited the content as needed and take full responsibility for the final manuscript

References

Ali, S., Nohra, C., Achkar, G.E., Faraj, J., & Khaled, M. (2025). Heat transfer, exergy, and cost: A sustainable analysis of concentric tube heat exchangers. Case studies in Thermal Engineering. https://doi.org/10.1016/j.csite.2025.105833

Birta, L., & Arbez, G.(2019). Modelling and Simulation Fundamentals. Modelling and Simulation. https://doi.org/10.1007/978-3-030-18869-6_2

Caldas, A. M. A., Ochoa, A. A. V., da Costa, J. A., Michima, P. S. A., Lima, Á. A. S., Leite, G. N. P., & Santos, C.A. C. (2021). Absorption refrigeration systems based on ammonia as refrigerant using different absorbents: Review and applications. Energies, 14(48), 48. https://doi.org/10.3390/en14010048

Carter, C., & Norton, M. (2012). Responding to Temperature Changes. 641-657. https://doi.org/10.1007/978-1-4614-3523-5_34

Chávez-Islas, L. M., Heard, C. L., & Grossmann, I. E. (2009). Synthesis and optimization of an ammonia–water absorption refrigeration cycle considering different types of heat exchangers by application of mixed-integer nonlinear programming. Industrial & Engineering Chemistry Research, 48(6), 2972–2990. https://doi.org/10.1021/ie801309h

Chen, X., Wang, R. Z., & Du, S. (2017). Heat integration of ammonia–water absorption refrigeration system through heat-exchanger network analysis. Energy, 141, 1585–1599. https://doi.org/10.1016/j.energy.2017.11.100

Dahal, R., Uusi-kyyny, P., Pokki, J.-P., & Alopaeus, V. (2023). Isobaric Vapor-Liquid Equilibrium of the Binary Mixtures Toluene + Styrene and Styrene + α-Methylstyrene. Journal of Chemical & Engineering Data. https://doi.org/10.1021/acs.jced.2c00662

Gmehling, J., Kleiber, M., Kolbe, B., & Rarey, J. (2019). Chemical Thermodynamics for process Simulation. https://doi.org/10.1002/9783527809479

Li, S., Zhenghao, J., Jiang, W., & Du, K. (2021). Experimental investigation of the effect of LiBr on the high-pressure part of a ternary working fluid ammonia absorption refrigeration system. Applied Thermal Engineering, 186, 116521. https://doi.org/10.1016/j.applthermaleng.2020.116521

Ningsih, E., Albanna, I., Witari, A. P., & Anggraini, G. L. (2022). Performance Simulation On The Shell And Tube Of Heat Exchanger By Aspen Hysys V.10. Jurnal Rekayasa Mesin. https://doi.org/10.21776/jrm.v13i3.1078

Sinnott, R., & Towler, G. (2020). Chemical Engineering Design (6th ed.). Butterworth-Heinemann.

Tahmid, M., & Syeda, S. (2023). A framework for integrating safety and environmental impact in the conceptual design of chemical processes. Pure and Applied Chemistry, 95, 301-314. https://doi.org/10.1515/pac-2022-1120

Thulukkanam, K. (2013). Heat Exchanger Design Handbook. https://doi.org/10.1201/b14877

Wang, S., Li, S., Xu, M., Jin, Z. and Xu, C. (2021). Simulation research on absorption refrigeration system based on NH3-H2O-LiBr vapor-liquid equilibrium calculation model. Thermal Science. doi: 10.2298/tsci210127201w.